Aspartic Acid 405 Contributes to the Substrate Specificity of Aminopeptidase B

Kayoko M. Fukasawa,*,‡ Junzo Hirose,§ Toshiyuki Hata,|| and Yukio Ono||

Department of Hard Tissue Research, Graduate School of Oral Medicine, Matsumoto Dental University, School of Dentistry, Shiojiri, Nagano 399-0781, Japan, Determent of Applied Biological Science, Faculty of Life Science and Biotechnology, Fukuyama University, Gakuen-cho, Fukuyama 729-0292, Japan, and Faculty of Pharmacy and Pharmaceutical Sciences, Fukuyama University, Gakuen-cho, Fukuyama 729-0292, Japan

Received March 8, 2006; Revised Manuscript Received July 13, 2006

ABSTRACT: Aminopeptidase B (EC 3.4.11.6, ApB) specifically cleaves *in vitro* the *N*-terminal Arg or Lys residue from peptides and synthetic derivatives. Ap B was shown to have a consensus sequence found in the metallopeptidase family. We determined the putative zinc binding residues (His324, His328, and Glu347) and the essential Glu325 residue for the enzyme using site-directed mutagenesis (Fukasawa, K. M., et al. (1999) *Biochem. J. 339*, 497−502). To identify the residues binding to the amino-terminal basic amino acid of the substrate, rat cDNA encoding ApB was cloned into pGEX-4T-3 so that recombinant protein was expressed as a GST fusion protein. Twelve acidic amino acid residues (Glu or Asp) in ApB were replaced with a Gln or Asn using site-directed mutagenesis. These mutants were isolated to characterize the kinetic parameters of enzyme activity toward Arg-NA and compare them to those of the wild-type ApB. The catalytic efficiency (k_{cat}/K_m) of the mutant D405N was 1.7×10^4 M^{-1} s^{-1}, markedly decreased compared with that of the wild-type ApB (6.2×10^5 M^{-1} s^{-1}). The replacement of Asp405 with an Asn residue resulted in the change of substrate specificity such that the specific activity of the mutant D405N toward Lys-NA was twice that toward Arg-NA (in the case of wild-type ApB; 0.4). Moreover, when Asp405 was replaced with an Ala residue, the k_{cat}/K_m ratio was 1000-fold lower than that of the wild-type ApB for hydrolysis of Arg-NA; in contrast, in the hydrolysis of Tyr-NA, the k_{cat}/K_m ratios of the wild-type (1.1×10^4 M^{-1} s^{-1}) and the mutated (8.2×10^3 M^{-1} s^{-1}) enzymes were similar. Furthermore, the replacement of Asp-405 with a Glu residue led to the reduction of the k_{cat}/K_m ratio for the hydrolysis of Arg-NA by a factor of 6 and an increase of that for the hydrolysis of Lys-NA. Then the k_{cat}/K_m ratio of the D405E mutant for the hydrolysis of Lys-NA was higher than that for the hydrolysis of Arg-NA as opposed to that of wild-type ApB. These data strongly suggest that the Asp 405 residue is involved in substrate binding via an interaction with the P1 amino group of the substrate's side chain.

The exopeptidase aminopeptidase B (ApB[1]; EC 3. 4. 11. 6), discovered in 1964 from a rat duodenal supernatant fraction (*1*) and originally identified in several rat tissues, specifically cleaves the *N*-terminal arginyl and lysyl residues from L-aminoacyl-β-naphthylamides (NA) and peptides such as kallidin. In 1996, ApB was cloned from rat liver as a 72.5 kDa protein containing 1 mol of zinc and was revealed to include an HEXXH consensus sequence commonly found in the zinc metallopeptidase family (*2*). It has been classified as a member of the aminopeptidase (Ap) family, which includes ApN (EC 3.4.11.2) (*3*), ApA (EC 3.4.11.7) (*4*), and leukotriene A_4 hydrolase (LTA4H; EC 3.3.2.6) (*5*) from mammals as well as several kinds of bacterial aminopeptidases. In particular, the amino acid sequence of ApB shows a high similarity to LTA4H from humans (37.2% identity) (*5*), rats (36.5% identity) (*6*), mice (37.3% identity) (*7*), and guinea pigs (38.1% identity) (*8*) and 22−25% identity with those of other Aps from mammals, such as ApN (*3*) and ApA (*4*). The 3D structure of ApB is unknown. However, on the basis of site-directed mutagenesis studies, we proposed that three amino acid residues (His324, His328, and Glu347) and a glutamic acid residue (325) in the HEXXH-18aa-E motif were involved in zinc coordination and catalytic activity (*9*), respectively, similar to the proposed roles of these residues in thermolysin (EC 3.4.24.4) as deduced from X-ray crystallography studies (*10*).

Aminopeptidases play critical roles in processes, such as protein maturation, protein digestion in its terminal stage, regulation of hormone levels, homeostatic protein turnover, and plasmid stabilization (*11*). These enzymes generally have broad substrate specificity. Of such enzymes, ApB specifically catalyzes the removal of *N*-terminal basic amino acids, and the rate of arginine release is typically about twice that of lysine (*12*). We set out to determine which amino acid residues in ApB contribute to substrate specificity. We presumed that certain acidic amino acid residues in ApB would be bound to the basic amino terminal of the substrate and sought them in this study. To do this, several acidic amino acid residues (Figure 1) in ApB were mutated to

* Corresponding author. Tel: 81-263-51-2073. Fax: 81-263-51-2199. E-mail: kmf@po.mdu.ac.jp.

‡ Matsumoto Dental University.

§ Department of Applied Biological Science, Fukuyama University.

|| Faculty of Pharmacy and Pharmaceutical Sciences, Fukuyama University.

[1] [1]Abbreviations: ApB, aminopeptidase B; ApA, aminopeptidase A; ApN, aminopeptidase N; LTA4H, leukotriene A_4 hydrolase; NA, L-aminoacyl-β-naphthylamide; 3D, three-dimensional; GST, glutathione S-transferase.

10.1021/bi0604577 CCC: $33.50
Published on Web 08/31/2006

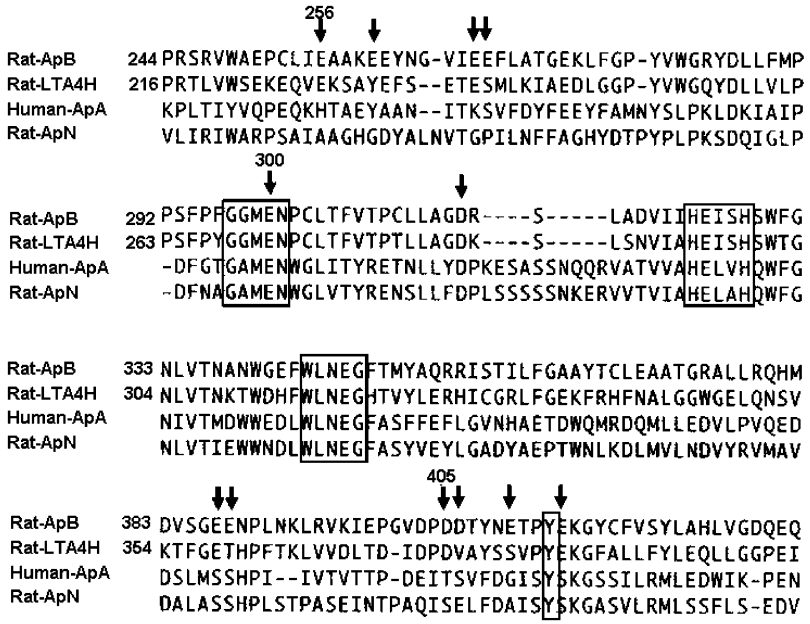

FIGURE 1: Alignment of the rat ApB amino acid sequence (*2*) with those of rat LTA4H (*6*), human ApA (*29*), and rat ApN (*3*). The mutated amino acid residues are denoted by arrows. The conserved motifs and tyrosyl residue in a mono-zinc aminopeptidase are shown by a box around those amino acid sequences.

neutral residues, and these mutants were purified and kinetically characterized to determine the substrate-binding residues. We based our hypothesis of the three-dimensional (3D) structure of ApB on the recently determined X-ray crystal structure of LTA4H (*13*).

EXPERIMENTAL PROCEDURES

Materials. Aminoacyl-NAs (Arg-, Lys-, Tyr-, Ala-, Gly-, Val-, Phe-, and Asp-) were obtained from Sigma. Restriction and modifying enzymes were from Toyobo Co. (Osaka, Japan). Oligonucleotides were synthesized by Hokkaido System Science Co., Ltd. (Sapporo, Japan). All other reagents were of analytical grade and were purchased from Nakarai Tesque (Kyoto, Japan) and Daiichi Chemicals (Tokyo, Japan).

Protein and Enzyme Assay. The purified enzyme concentrations were calculated using an extinction coefficient at 280 nm, $E^{1\%}$ of 22.5. Enzyme activity using aminoacyl-NA as the substrate was measured by a slight modification of the method of Hopsu et al. (*14*). The incubation mixture comprised 10 μmol of Tris-HCl buffer (pH 7.5) containing 15 μmol of NaCl, 0.04 μmol of the substrate, and an appropriate amount of enzyme plus water to 200 μL. After incubation at 37 °C for 20 min, 500 μL of 1 M acetate buffer (pH 4.0) containing 10% Tween 20 and 200 μL of Fast Garnet GBC (0.2 mg/mL of H_2O) were added to the reaction mixture. The absorbance of the resulting diazo dye was measured at 530 nm.

Enzyme Kinetics. For curve fitting by nonlinear regression and calculation of V_{max} and K_m, the program KaleidoGraph (Hulinks, Tokyo, Japan) was used. The amounts of substrates used in these kinetic studies ranged from 0.05 to 1.0 mM for Arg-NA, Lys-NA, and Tyr-NA. The k_{cat} values were calculated on the basis of a molecular mass of 72 545 Da calculated from the deduced amino acid sequence of rat ApB.

SDS−Polyacrylamide Gel Electrophoresis (SDS−PAGE). The purity of the purified mutated enzymes was determined by SDS−PAGE as described by Laemmli (*15*). An appropriate amount of the purified enzyme was added to an equal volume of sample buffer containing 4% SDS and 2% 2-mercaptoethanol, boiled for 5 min, and then used. A uniform polyacrylamide slab gel (10%) with a 5% stacking gel was run at room temperature until bromphenol blue reached the bottom of the slab. The gel was then stained with Coomassie Brilliant Blue R250.

Site-Directed Mutagenesis and Cloning. Site-directed mutagenesis was performed on cDNA encoding rat ApB with a Quick Change Multi Site-Directed Mutagenesis Kit from Stratagene by polymerase chain reaction, according to the manufacturer's recommended protocol. The pBluescript phagemid (SK) containing cDNA encoding rat ApB was constructed as described previously (*2*). The two primers for changing the two *EcoRI* restriction sites of rat ApB cDNA and the appropriate mutagenic primer (Figure 1, Table 1) were annealed and extended by 30 cycles of polymerase chain reaction. After restriction digestion with *DpnI*, the mutated product transformed repair-deficient *mutS Escherichia coli* (XL*mutS* competent cells), and the transformed cells were selected by growth on ampicillin. The recombinant phagemid was purified using QIAprep Spin Miniprep, and the presence of the mutation and nonspecific mutations were confirmed by automated sequencing using Applied Biosystems PRISM 310NT Genetic Analyzer. For expressing the recombinant protein as a glutathione S-transferase (GST) fusion protein, the mutated cDNA isolated from the recombinant mutated phagemid was subcloned into pGEX-4T-3 (Amersham Pharmacia Biotech) digested with *Eco*RI-*Xho*I.

Expression and Purification of Recombinant ApB Mutants. Mutated enzymes were expressed as GST fusion proteins in *Escherichia coli* BL21 cells grown at 28 °C in 2 × YTA (1.6% trypton, 1.0% yeast extract, 0.5% NaCl) supplemented with 100 μg/mL of ampicillin. At A_{620} = 0.2, isopropyl-β-D-thiogalacto-pyranoside was added to a final concentration of 200 μM. After incubation for another 4 h at 28 °C, the

Table 1: Primers Used for the Mutagenesis of Rat ApB cDNA

mutation	nucleotide sequence	numbering
	changing restriction sites	
EcoRI site 1	5′-CTGGGGGGAGTTCTGGCT-3′	1017 → 1035
EcoRI site 2	5′-CTTTCTGGAGTTCTACCTG-3′	1359 → 1377
	mutagenic primers	
Glu256 → Gln	5′-CCTGCCTGATTCAAGCCGCCAAGG-3′	755 → 778
Glu260 → Gln	5′-GAAGCCGCCAAGCAGGAATACAATGG-3′	766 → 791
Glu267 → Gln	5′-GGGGTCATACAAGAATTTCTGG′C-3′	789 → 812
Glu268 → Gln	5′-GGGTCATAGAACAATTTCTGGCAAC-3′	790 → 815
Glu300 → Gln	5′-CCGTTTGGAGGAATGCAGAATCCCTGCCTG-3′	882 → 910
Asp315 → Asn	5′-CTAGCAGGAACCGCTCCTTAG-3′	934 → 955
Glu387 → Gln	5′-GTGTCTGGACAGGAAAACCC-3′	1150 → 1169
Glu388 → Gln	5′-GTCTGGAGAGCAAAACCCAC-3′	1152 → 1171
Asp405 → Ala	5′-GGTGTTGACCCAGCTGACACCTACAATG-3′	1201 → 1224
Asp405 → Glu	5′-GTGTTGACCCAGAAGACACCTACAATG-3′	1202 → 1224
Asp405 → Asn	5′-GGTGTTGACCCAAATGACACCTAC-3′	1201 → 1220
Asp406 → Asn	5′-TTGACCCAGATAACACCTACAATG-3′	1205 → 1220
Glu410 → Gln	5′-GACACCTACAATCAAACCCCCTACG-3′	1216 → 1240
Glu414 → Gln	5′-CCCCCTACCAGAAAGGTTAC-3′	1232 → 1251

cells were collected from centrifugation at 20 000*g* for 10 min. The cell pellet was resuspended in 80 mL of PBS containing benzamidine (5 mM) and iodoacetic acid (1 mM) and lysed using ultrasonic treatment at 9 kHz for 1 min, repeated three times at intervals of 5 min. A clear supernatant fluid was obtained by centrifugation at 250 000*g* for 45 min and then loaded into a glutathione−Sepharose 4B column (1.0 × 3.0 cm, from Amersham Pharmacia Biotech). After the column was washed with 100 mL of PBS, 1 mL of thrombin solution (50 units/mL) was loaded onto the column and incubated at 4 °C for 2 h, and the proteins were eluted with 1 × PBS at 4 °C. The eluted fractions were immediately supplemented with benzamidine (5 mM), concentrated to 1.0 mL, and loaded onto a Sephadex G-150 column (1.0 × 80 cm) equilibrated with 50 mM Tris-HCl at pH 8.2, containing 50 mM NaCl. For the wild-type ApB, the enzyme fractions were determined by hydrolyzing Arg-NA activity and absorbance at 280 nm. The mutated enzyme peak was identified as having the same fractions as that of the wild-type ApB peak on a Sephadex G-150 column. The purified proteins were concentrated to 500 μL and mixed with an equal volume of 50% glycerol and stored at −20 °C until use.

Docking Simulation of the Adduct of Arg-NA with LTA4H. The AutoDock 3.0.5 docking program (*16*) was used for the present investigation. The crystal structure of LTA4H and zinc ions were extracted from the crystal structure of the LTA4H complex with bestatin (pdb code: 1HS6; 1.95 Å resolution) (*13*) obtained from the Protein Data Bank. The polar hydrogen, partial atomic charge, and solvation parameters for use with the AutoDock simulation were applied using AutoDockTools (*17*). The geometry of Arg-NA as a ligand molecule in the present study was optimized by the semiempirical MNDO−AM1 method (*18*). However, the partial atomic charges of the ligand molecules were added as the Gasteiger charges by AutoDockTools programs.

The docking simulation calculations were carried out with a rigid LTA4H and a flexible ligand. Then, a suitable structure for flexible ligands was determined by rotation of the ligand molecule's C−C and C−N single bonds, other than the peptide bond. The grid parameter file (input file for AutoGrid) and the docking parameter file (input file for AutoDock) were set up by the AutoDockTools program. A grid of 127 × 127 × 127 points in the *x*-, *y*-, and *z*-axis directions was built, and the grid center was situated in the center of LTA4H. Default settings were used for all other parameters.

Docking simulations were carried out by AutoDock using a Lamarckian genetic algorithm and were repeated 100 times. At the end of the docking simulation, the ligand−LTA4H complex with the most stable energy was adopted as the most favorable structure of the complex for LTA4H. All calculations were carried out on the NEC PC-Cluster system from the Green Science Research Center at Fukuyama University.

RESULTS

Mutagenic Replacement, Expression, and Purification of Recombinant Proteins. We replaced the acidic amino acid in ApB Glu256, 260, 267, 268, 300, 387, 388, 410, or 414 with a Gln residue, Asp315 or 406 with an Asn residue, and Asp405 with an Asn, Ala, or Glu residue by site-directed mutagenesis. The mutated amino acid residues are shown on the amino acid sequence of ApB in Figure 1. The resulting 14 mutants and the wild-type enzymes were all expressed as GST-fusion proteins in *Escherichia coli* to allow for rapid purification on a glutathione-Sepharose 4B column. The level of expression was similar for the wild-type enzyme and all mutants with a final yield of about 100−500 μg of protein per liter of cell culture. These mutated proteins were purified to apparent homogeneity and behaved like the wild-type enzyme (Figure 2). The purified mutated enzymes D405N and D405E were so extremely unstable that 90% of their aminopeptidase activities were lost during 10 days at 0 °C. The other mutants and the wild-type enzyme kept these hydrolyzing activities longer than 1 month at 0 °C.

Kinetic Parameters for Mutants Replacing an Acidic Amino Acid with a Noncharged Residue for Hydrolysis of Arg-NA. For these mutants, except for E300Q, D405N, E410Q, and E414Q, the K_m values and the k_{cat}/K_m ratios ranged between 34% and 140% and between 30% and 106% of those of the wild-type enzyme, respectively. For the D405N, E410Q, and E414Q mutants, the catalytic efficiency (k_{cat}/K_m) was significantly lower ($\times 10^{-1}$) than that for the wild-type enzyme, and the replacement of Glu300 eliminated the Arg-NA hydrolyzing activity (Table 2).

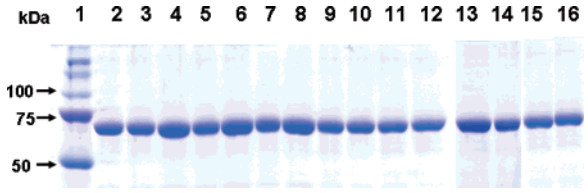

FIGURE 2: SDS−PAGE of wild-type and mutated ApB proteins. Wild-type ApB (lane 2), and mutated proteins E256Q (lane 3), E260Q (lane 4), E267Q (lane 5), E268Q (lane 6), E300Q (lane 7), D315N (lane 8), E387Q (lane 9), E388Q (lane 10), D405N (lane 11), D405E (lane 12), D405A (lane 13), D406N (lane 14), E410Q (lane 15), and E414Q (lane 16) (2∼3 μg each), underwent electrophoresis on a standard 10% gel and were stained with Coomassie Brilliant Blue. Molecular mass markers (kDa) are shown in lane 1.

Table 2: Kinetic Parameters for Wild-Type and Mutated ApBs[a]

	K_m ($\times 10^{-5}$ M)	k_{cat} (s^{-1})	k_{cat}/K_m ($M^{-1}\,s^{-1}$)
wild type	8.8 ± 1.3	54.1 ± 2.5	6.2×10^5
E256Q	9.9 ± 2.7	51.8 ± 2.4	5.2×10^5
E260Q	6.2 ± 1.4	12.0 ± 0.9	1.9×10^5
E267Q	11.9 ± 2.0	24.1 ± 0.6	2.0×10^5
E268Q	6.4 ± 0.6	11.7 ± 0.5	1.8×10^5
E300Q		ND[b]	
D315N	12.5 ± 1.4	38.0 ± 2.9	3.0×10^5
E387Q	10.9 ± 0.8	60.0 ± 1.4	5.6×10^5
E388Q	11.1 ± 2.3	53.3 ± 1.5	4.8×10^5
D405N	12.3 ± 1.2	2.1 ± 0.03	1.7×10^4
D406N	3.0 ± 0.5	19.6 ± 0.7	6.6×10^5
E410Q	12.8 ± 2.8	6.3 ± 0.5	5.0×10^4
E414Q	38.4 ± 1.8	13.5 ± 0.3	3.5×10^4

[a] Data are the means ± SD of two separate experiments with duplicate determinations. [b] Not detectable.

Effects of the Replacement of Asp405 with an Ala or Glu Residue. Table 3 shows the relative rates of hydrolyzing activities toward aminoacyl-β-naphthylamide derivatives of the D405N, E410Q, and E414Q mutants, which exhibited significantly lower k_{cat}/K_m ratios for the hydrolysis of Arg-NA. Only the replacement of Asp405 with an Asn residue resulted in the change of substrate specificity. The relative activity of the D405N mutant for the hydrolysis of Lys-NA was twice that for the hydrolysis of Arg-NA; furthermore, that for the hydrolysis of Phe-NA or Tyr-NA also increased compared with those of the wild-type enzyme (Table 3).

The kinetic parameters of the D405A and D405E mutants for the hydrolysis of Arg-NA, Lys-NA, or Tyr-NA are shown in Table 4. For the replacement of Asp405 with an Ala residue, the K_m value for the hydrolysis of Arg-NA was six times higher, and the k_{cat}/K_m ratio was 10^3 times smaller than those of the wild-type enzyme. Furthermore, the K_m value and the k_{cat}/K_m ratio for the hydrolysis of Lys-NA were markedly reduced by factors of 10^2 and 5×10^3, respectively. In contrast, the kinetic parameters for the hydrolysis of Tyr-NA were similar to those of the wild-type enzyme. For the D405A mutant, Tyr-NA was the most adaptable substrate.

When Asp405 was replaced with the acidic amino acid residue Glu, the K_m value for the hydrolysis of Arg-NA was not significantly affected, whereas the k_{cat}/K_m ratio was reduced by a factor of 6; in contrast, for the hydrolysis of Lys-NA, the k_{cat}/K_m ratio of the D405E mutant was increased by a factor of 1.6 (Table 4). The k_{cat}/K_m ratio of the D405E mutant for the hydrolysis of Lys-NA was higher than that for the hydrolysis of Arg-NA (Table 4).

AutoDock Simulations of the Arg-NA−LTA4H Complex. At first, the degree of confidence for the AutoDock 3.0.5 program used in the present study was examined by the results calculated by the docking simulation for the Bestatin−LTA4H complex. The reliability of the AutoDock program was confirmed by the fact that the structure of the Bestatin−LTA4H complex (interaction mode) calculated by the Autodock 3.0.5 program coincided very well with the result of the experimental X-ray crystal structure analysis.

The most favorable interaction mode of Arg-NA with LTA4H was obtained by the results of the docking simulation in this study. This interaction mode at the catalytic site center is shown in Figure 3. As to this interaction mode between the zinc ion, guanidino, and terminal amino groups of Arg-NA and the amino acid residues of LTA4H, Figure 3 clearly shows the following two points. First, the oxygen atom from the carbonyl group of Arg-NA was spatially directed to the zinc ion, and the interatomic distance between the oxygen and zinc atoms was 2.03 Å. Second, the Asp375 residue formed a hydrogen bond with the guanidino group of Arg-NA. However, Glu271 and Gln136 residues formed hydrogen bonds with the terminal amino group. As shown in Figure 3, the interatomic distances of interactions for Asp375 with the guanidino group and for Glu271 and Gln136 with terminal amino group, were 2.77, 2.73−2.74, and 2.78 Å, respectively.

DISCUSSION

ApB is a zinc-dependent enzyme containing a conserved HEXXH-18aa-E motif involved in catalytic activity as shown by molecular cloning and site-directed mutagenesis (*2*, *9*). In addition, ApB contains another motif, GXMEN, found in members of the monozinc aminopeptidase family. Site-directed mutagenesis of the glutamate of the GXMEN motif in ApA, ApN, and LTA4H showed that this residue was implicated in the exopeptidase specificity of aminopeptidase (*19*, *20*, *21*) (Figure 1). In the case of ApB, the exchange of Glu for a Gln residue in the GXMEN motif of ApB resulted in a nonmeasurable activity (Table 2); hence, we predicted that the glutamate of the GXMEN motif in ApB might be implicated in substrate binding during catalysis by interacting with the free *N*-terminal part of substrates.

ApB specifically cleaves the *N*-terminal arginyl or lysyl residue from either the peptide or the chemosynthetic substrate. We predicted that the S1 subsite of ApB would be electronegatively charged and interact with the P1 side-chain amino group of the substrate. Figure 1 shows the alignment of the rat ApB amino acid sequence with those of other monozinc aminopeptidases and the positions of the acidic amino acid, glutamate, or aspartate residues in ApB that were replaced with noncharged amino acid residues. A comparison of the amino acid sequence of ApB with several monozinc aminopeptidases revealed that LTA4H, a bifunctional enzyme with both epoxide hydrolase and aminopeptidase activity, was the structurally closest molecule to ApB (*2*, *22*) (Figure 1). The Arg-NA hydrolyzing activities of the ApB mutants D405N, E410Q, and E414Q were decreased (Table 2). On the basis of the recently determined X-ray crystal structure of LTA4H, the amino acid residues Asp375, Ser380, and Glu384 in LTA4H, corresponding to Asp405, Glu410, and Glu414 in ApB, respectively, are located in the

Table 3: Specific Activities of Wild-Type, D405N, E410Q, and E414Q ApBs for the Hydrolysis of Various Aminoacyl-β-Naphthylamide Derivatives[a]

	μmol/mg of protein (relative rate of hydrolysis[b]/%)			
substrate	wild type	D405N	E410Q	E414Q
Arg-NA	33.9 ± 2.5 (100)	1.12 ± 0.09 (100)	2.51 ± 0.10 (100)	3.81 ± 0.21 (100)
Lys-NA	13.9 ± 0.5 (41)	2.33 ± 0.21 (208)	0.551 ± 0.010 (22)	0.512 ± 0.011 (13)
Ala-NA	0.034 ± 0.001 (0.1)	ND[c]	ND	ND
Gly-NA	<0.02	ND	ND	ND
Val-NA	0.034 ± 0.002 (0.1)	ND	ND	ND
Phe-NA	0.171 ± 0.010 (0.5)	0.364 ± 0.021 (33)	ND	ND
Tyr-NA	0.171 ± 0.010 (0.5)	0.364 ± 0.027 (33)	ND	ND
Asp-NA	ND	ND	ND	ND

[a] Data are the means ± SD of two separate experiments with duplicate determinations. [b] Relative rate of hydrolysis: the value of 100 was given to Arg-NA. [c] Not detectable.

Table 4: Kinetic Parameters of Wild-Type, D405A, and D405E ApBs for the Hydrolysis of Arg-, Lys-, or Tyr-β-naphthylamide[a]

	substrate	K_m ($\times 10^{-5}$ M)	k_{cat} (s^{-1})	k_{cat}/K_m ($M^{-1}s^{-1}$)
wild type	Arg-NA	8.8 ± 1.3	54.1 ± 2.5	6.2×10^5
	Lys-NA	14.0 ± 2.1	23.6 ± 1.8	2.3×10^5
	Tyr-NA	19.7 ± 5.2	2.1 ± 0.3	1.1×10^4
D405A	Arg-NA	57.8 ± 6.3	0.49 ± 0.03	8.4×10^2
	Lys-NA	1690 ± 360	0.83 ± 0.13	4.9×10
	Tyr-NA	12.4 ± 1.2	1.00 ± 0.10	8.2×10^3
D405E	Arg-NA	10.5 ± 1.6	11.5 ± 0.6	1.0×10^5
	Lys-NA	21.3 ± 1.9	79.3 ± 2.7	3.7×10^5
	Tyr-NA	ND[b]		

[a] Data are the means ± SD of two separate experiments with duplicate determinations. [b] Not detectable.

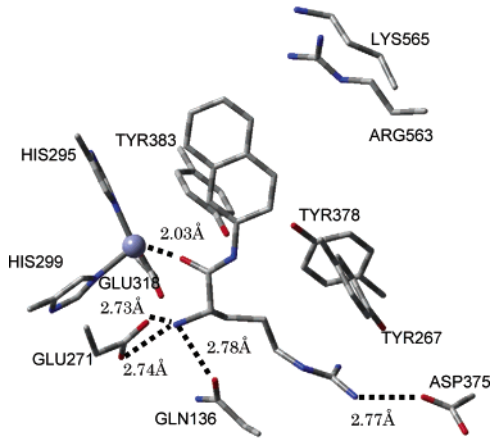

FIGURE 3: Most favorable interaction mode of Arg-NA with LTA4H obtained from a docking simulation using Autodock 3.0.5. Carbon, nitrogen, and oxygen atoms are colored in gray, blue, and red, respectively; the zinc ion is shown as a purple sphere. The carbonyl group of Arg-NA is bound to the zinc ion. The interatomic distance between the oxygen of the carbonyl group and the zinc atom is 2.03 Å. The terminal amino group of Arg-NA is bound to GLN136 and GLU271. In addition, the guanidino group of Arg-NA is bound to ASP375 in LTA4H. Because the distances between the nitrogen atoms of these groups in Arg-NA and corresponding oxygen atoms of amino acid residues in LTA4H are 2.73−2.78 Å, these interactions are hydrogen bonding interactions.

putative substrate binding cavity containing the glutamate residues in the conserved motifs (GXME[271]N and HE[296]XXH), (*13*, *23*). These results suggest that the 3D structure of ApB may be similar to that of LTA4H. The other residues, Glu256, Glu260, Glu267, Glu268, and Asp315 in ApB, whose mutations were barely influenced by those enzyme activities, corresponding to Glu228, Tyr232, Glu238, Glu239, and Asp286 in LTA4H, respectively, are speculated to be remote from the putative substrate binding cavity on the basis of the X-ray crystal structure of LTA4H. Moreover, Asp406, Glu387 and Glu388 in ApB, corresponding to Val376, Glu358, and Thr359 in LTA4H, respectively, might be located in the putative substrate binding cavity or close to the catalytic domain; nevertheless, those side chains of the Val376, Glu358, and Thr359 in LTA4H might be outside the putative substrate binding pocket. It is reasonable that the activities of these mutants (E265Q, E260Q, E267Q, E268Q, D315N, E387Q, E388Q, and D406N) were not significantly changed.

For the E410Q and E414Q mutants, the catalytic efficiency was also lower ($\times 10^{-1}$), similar to that for the D405N mutant. These two glutamate residues are close to the Tyr408 and Tyr413 residues in ApB. The Tyr378 and Tyr383 residues in LTA4H (Figure 3), corresponding to the Tyr408 and Tyr413 residues in ApB, are involved in catalytic activity for epoxide hydrolase (*24*) and peptidase (*25*), respectively (Figure 3). Furthermore, the Tyr471 residue in ApA, corresponding to the Tyr413 residue in ApB, has been shown to participate in catalysis by stabilizing the transition state complex (*26*). Hence, the replacement of Glu410 or Glu414 with a glutamine residue in ApB may decrease the activity by changing the 3D structure of the active domain.

The replacement of Asp405 with an Ala residue by site-directed mutagenesis resulted in a markedly decreased k_{cat}/K_m ratio for the hydrolysis of Arg-NA, 10^{-3} times lower than that of the wild-type enzyme (Table 4); in contrast, the k_{cat}/K_m ratios for the hydrolysis of Tyr-NA of the D405A and the wild-type ApBs were approximately the same. Thus, Asp405 in ApB may be interconnected with the positive charge of the guanidine part of Arg-NA.

When Asp405 was replaced with a Glu residue, an amino acid with similar polarity but one that adds length to the side chain of the Asp405, the ratio of the k_{cat}/K_m ratio for the hydrolysis of Arg-NA to that for the hydrolysis of Lys-NA was changed from three times to one-third. Figure 4 models the relationships between the substrate, Arg-NA (Figure 4a) or Lys-NA (Figure 4b), and the putative active domain of the wild-type enzyme (Figure 4a) and the D405E mutated enzyme (Figure 4b), respectively. The putative substrate binding pocket may be remarkably tight because the replacement of Asp405 with an asparaginyl or glutamate residue adds one nitrogen or carbon atom to the side chain of the aspartic acid, decreasing the enzyme stability of ApB. Thus, Lys-NA may be a more suitable substrate than Arg-

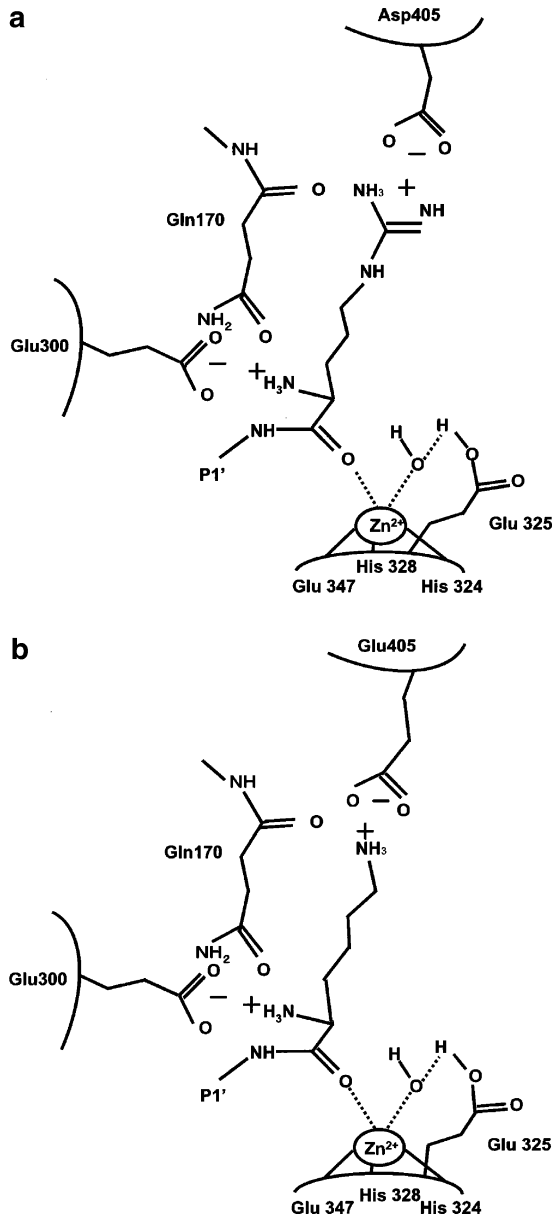

FIGURE 4: Models for the relationships between substrate and ApB. (a) Arg-NA and the predicted S1 subsite and putative active domain of the wild-type enzyme. (b) Lys-NA and predicted S1 subsite and putative active domain of the D405E mutated enzyme. The guanidine in the substrate is bound to the negatively charged Asp405 in the wild-type ApB (a) and the amino group in the substrate bound to Glu405 in the mutant D405E (b). Gln170 and Glu300 in ApBs are bound to the *N*-terminal amine of the substrate.

NA for the D405E mutant, adding one carbon atom to the side chain of the Asp405 residue in ApB (Figure 4b). These results show that Asp 405 in ApB may be bound to the substrate's P1 side-chain basic amine. In contrast, Gln170 and Glu300 of ApB, corresponding to Gln136 and Glu271 of LTA4H may be involved in recognizing the N terminal of Arg-NA or Lys-NA (Figure 3).

The Asp375 residue, corresponding to Asp405 of ApB, was one of the polar residues involved in the complex of LTA4H with Bestatin (*13*). Furthermore, in a site-directed mutagenesis experiment, Asp375 was shown to be a catalytic residue specifically required for the epoxide hydrolase reaction and not for aminopeptidase activity (*27*). The role of Asp405 in ApB may be the recognition of the positive charge of guanidino or amino group in the substrate, Arg-NA or Lys-NA.

We performed a docking simulation of LTA4H with Arg-NA using the automated docking tools of AutoDock 3.0. In Figure 3, it is shown that an oxygen atom of the side chain of Asp375 bound to the guanidine part of Arg-NA and Gln136 bound to the *N*-terminal amine of Arg-NA are involved in the substrate interaction in LTA4H. The results confirmed that the Asp405 residue in ApB corresponding to Asp375 in LTA4H may be constituted in the active site of the enzyme and give a negative charge to the S1 subsite for binding to the positively charged *N*-terminal amino acid residue of the substrate. Also, the Gln170 in ApB, corresponding to Gln136 in LTA4H, may be involved in recognizing the N terminal of the substrate.

More recently, X-ray crystal structure analysis and mutation experiments of LTA4H (*28*) have suggested that the Arg563 and Lys565 residues are carboxylate recognition sites for the epoxide hydrolase and aminopeptidase substrates. In particular, all mutants replacing Arg563 (R563K, R563A, and R563M), corresponding to Lys599 of ApB, lack epoxide hydrolase activity. These results demonstrate that ApB does not possess epoxide hydrolase activity as previously described by Fukasawa et al. (*9*). In Figure 3, the aromatic ring of naphthylamide of the Arg-NA is oriented to Arg563 and Lys565. The shortest length between an N atom of the guanidine group of the Arg563 residue and a C atom of the aromatic ring of naphthylamide in Arg-NA is about 3.3 Å. Rundberg, P. C. et al. (*28*) proposed that Arg563 and Lys565 residues in LTA4H recognize the negative charge of the C terminal of the peptide substrate. Arg563 and Lys565 residues in LTA4H correspond to Lys599 and Lys601 in ApB. These plus-charged residues, Lys599 and Lys601 in ApB, may also be involved in recognizing the C terminal of the peptide substrates.

REFERENCES

1. Hopsu, V. K., Kantonen, U.-M., and Glenner, G. G. (1964) A peptidase from rat tissues selectively hydrolysing N-terminal arginine and lysine residues, *Life Sci. 3* 1449−1453.
2. Fukasawa, K. M., Fukasawa, K., Kanai, M., Fujii, S., and Harada, M. (1996) Molecular cloning and exression of rat liver aminopeptidase B, *J. Biol. Chem. 271*, 30731−30735.
3. Watt, V. M., and Yip, C. C. (1989) Amino acid sequence deduced from a rat kidney cDNA suggests it encodes the Zn-peptidase aminopeptidase N, *J. Biol. Chem. 264*, 5480−5487.
4. Wu, Q., Lahti, J. M., Air, G. M., Burrows, P. D., and Cooper, M. D. (1990) Molecular cloning of the murine BP-1/6C3 antigen: a member of the zinc-dependent metallopeptidase family, *Proc. Natl. Acad. Sci. U.S.A. 87*, 993−997.
5. Minami, M., Ohno, S., Kawasaki, H., Rådmark, O., Samuelsson, B., Jörnvall, H., Shimizu, T., Seyama, Y., and Suzuki, K. (1987) Molecular cloning of a cDNA coding for human leukotriene A4 hydrolase. Complete primary structure of an enzyme involved in eicosanoid synthesis, *J. Biol. Chem. 262*, 13873−13876.
6. Makita, N., Funk, C. D., Imai, E., Hoover, R.-L., and Badr, K. F. (1992) Molecular cloning and functional expression of rat leukotriene A4 hydrolase using the polymerase chain reaction, *FEBS Lett. 299*, 273−277.
7. Medina, J. F., Rådmark, O., Funk, C. D., and Haeggström, J. Z. (1991) Molecular cloning and expression of mouse leukotriene A4 hydrolase cDNA, *Biochem. Biophys. Res. Commun. 176*, 1516−1524.
8. Minami, M., Mutoh, H., Ohishi, N., Honda, Z., Bito, H., and Shimizu, T. (1995) Amino-acid sequence and tissue distribution of guinea-pig leukotriene A4 hydrolase, *Gene 161*, 249−251.
9. Fukasawa, K. M., Fukasawa, K., Harada, M., Hirose, J., Izumi, T., and Shimizu, T. (1999) Aminopeptidase B is structurally

related to leukotriene-A4 hydrolase but is not a bifunctional enzyme with epoxide hydrolase activity, *Biochem. J. 339*, 497−502.
10. Matthews, B. W. (1988) Structural basis of the action of thermolysin and related zinc peptidase, *Acc. Chem. Res. 21*, 333−340.
11. Taylor, A. (1993) Aminopeptidases: towards a mechanism of action, *Trends Biochem. Sci. 18*, 167−172.
12. McDonald, J. K., and Barrett, A. J. (1986) Soluble Arginyl Aminopeptidase, in *Mammalian Proteases* (McDonald, J. K., and Barrett, A. J., Eds), Vol. 2, pp. 48−55, Academic Press, Inc., London.
13. Thunnissen, M. M. G. M., Nordlund, P., and Haeggström, J. Z. (2001) Crystal structure of human leukotriene A4 hydrolase, a bifunctinal enzyme in inflammation, *Nat. Struct. Biol. 8*, 131−135.
14. Hopsu, V. K., Mäkinen, K. K., and Glenner, G. G. (1966) Purification of mammalian peptidase selective for N-terminal arginine and lysine residues: aminopeptidase B, *Arch. Biochem. Biophys. 114*, 557−566.
15. Laemmli, U. K. (1970) Cleavage of structural proteins during the assembly of the head of bacteriophage T4, *Nature 227*, 680−685.
16. Morris, G. M., Goodsell, D. S., Halliday, R. S., Huey, R., Hart, W. E., Belew, R. K., Olson, A. J. (1998) Automated docking using a Lamarckian genetic algorithm and an empirical binding free energy function, *J. Comput. Chem. 19*, 1639−1662.
17. *AutoDockTools*, http://www.scripps.edu/%7Esanner/python/index.html.
18. Dewar, M. J. S., Zoebisch, E. G., Healy, E. F., and Stewart, J. J. P. (1985) Development and use of quantum mechanical molecular models. 76. AM1: a new general purpose quantum mechanical molecular model, *J. Am. Chem. Soc. 107*, 3902−3909.
19. Vazeux, G., Iturrioz, X., Corvol, P., and Llorens-Cortes, C. (1998) Aglutamate residue contributes to the exopeptidase specificity in aminopeptidase A, *Biochem. J. 334*, 407−413.
20. Luciani, N., Marie-Claire, C., Ruffet, E., Beaumont, A., Roques, B. P., and Fournie-Zaluski, M.-C. (1998) Characterization of Glu350 as a critical residue involved in the N-terminal amine binding site of aminopeptidase N (EC 3.4.11.2): insights into its mechanism of action, *Biochemistry 37*, 686−692.
21. Rudberg, P. C., Tholander, F., Thunnissen, M. M. G. M., and Haeggström, J. Z. (2002) Leukotriene A4 hydrolase/aminopeptidase. Glutamate 271 is a catalytic residue with specific roles in two distinct enzyme mechanisms, *J. Biol. Chem. 277*, 1398−1404.
22. Cadel, S., Foulon, T., Viron, A., Balogh, A., Midol-Monnet, S., Noel, N., and Cohen, P. (1997) Aminopeptidase B from rat testis is a bifunctional enzyme structurally related to leukotriene-A4 hydrolase, *Proc. Natl. Acad. Sci. U.S.A. 94*, 2964−2968.
23. Thunnissen, M. M. G. M., Andersson, B., Samuelsson, B., Wong, C.-H., and Haeggström, J. Z. (2002) Crystal structures of leukotriene A4 hydrolase in complex with captopril and two competitive tight-binding inhibitors, *FASEB J. 16*, 1648−1650.
24. Mueller, M. J., Blomster, M., Oppermann, U. C. T., Jörnvall, H., Samuelsson, B., and Haeggström, J. Z. (1996) Leukotriene A4 hydrolase: Protection from mechanism-based inactivation by mutation of tyrosine-378, *Proc. Natl. Acad. Sci. U.S.A. 93*, 5931−5935.
25. Blomster, M., Wetterholm, A., Mueller, M. J., and Haeggström, J. Z. (1995) Evidence for a catalytic role of tyrosine 383 in the peptidase reaction of leukotriene A4 hydrolase, *Eur. J. Biochem. 231*, 528−534.
26. Vazeux, G., Iturrioz, X., Corvol, P., and Llorens-Cortes, C. (1997) A tyrosine residue essential for catalytic activity in aminopeptidase A, *Biochem. J. 327*, 883−889.
27. Rudberg, P. C., Tholander, F., Thunnissen, M. M. G. M., Samuelsson, B., and Haeggström, J. Z. (2002) Leukotriene A4 hydrolase: selective abrogation of leukotriene B4 formation by mutation of aspartic acid 375, *Proc. Natl. Acad. Sci. U.S.A. 99*, 4215−4220.
28. Rudberg, P. C., Tholander, F., Andberg, A., Thunnissen, M. M. G. M., and Haeggström, J. Z. (2004) Leukotriene A4 hydrolase: Identification of common carboxylate recognition site for the epoxide hydrolase and aminopeptidase substrates, *J Biol. Chem. 279*, 27376−27382.
29. Nanus, D. M., Engelstein, D., Gastl, G. A., Gluck, L., Vidal. M. J., Morrison, M., Finstad, C. L., Bander, N. H., and Albino, A. P. (1993) Molecular cloning of the human kidney differentiation antigen gp160: human aminopeptidase A, *Proc. Natl. Acad. Sci. U.S.A. 90*, 7069−7073.

BI0604577